1979.
3. B. R. Judd, *Phys. Rev.*, **127**, 750 (1962).
4. G. S. Ofelt, *J. Chem. Phys.*, **37**, 511 (1962).
5. R. D. Peacock, Struct. Bonding, Vol. 22, p. 83, edited by J. D. Dunitz, Springer-Verlag, Berlin Heideberg, New York, 1975.
6. E. M. Stephens, S. Davis, M. F. Reid, and F. S. Richardson, *Inorg. Chem.*, **23**, 4607 (1984).
7. M. T. Devlin, E. M. Stephens, F. S. Richardson, T. C. Van Cott, and S. A. Davis, *Inorg. Chem.*, **26**, 1204 (1987).
8. S. A. Davis and F. S. Richardson, *Inorg. Chem.*, **23**, 184 (1984).
9. M. T. Devlin, E. M. Stephens, and F. S. Richardson, *Inorg. Chem.* **27**, 1517 (1988).
10. W. T. Carnall, P. R. Fields, and K. Rajnak, *J. Chem. Phys.*, **49**, 4412 (1968).
11. A. E. Martell and R. M. Smith, Critical Stability Constants, Vol. 1-3, Plenum Press, New York and London (1977).

An Explanation of the Contrasting Reactivities of *meso*- and *d,l*-D_3-Trishomocubylidene-D_3-trishomocubane towards Electrophiles

Oh Seuk Lee* and Eiji Ōsawa†

Department of Chemistry, Andong National University, Kyoungpuk 760-749
†Department of Knowledge-Based Information Engineering,
Toyohashi University of Technology, Toyohashi 441, Japan. *Received September 24, 1991*

The contrasting behaviour of *meso*- and *d,l*-D_3-trishomocubylidene-D_3-trishomocubane (**1** and **2**) in the electrophilic addition reaction, the former giving rearranged spiro compound (**1a** and **1b**) and the latter giving 1,2-adduct (**2a** and **2b**), has been explained as arising from the secondary steric effects based on computational evidence. As the degree of out-of-plane deformation of the olefinic carbon atoms increases with reaction progress, the resulting internal congestion in the region behind the double bond becomes unbearably large in *meso*-**1**. The absence of symmetry plane across the double bond of *d,l*-**2** helps for the closing fragments to adjust themselves.

Introduction

The reaction of a mixture of *meso*-dimer (**1**) of D_3-trishomocubanone and corresponding *d,l*-dimer (**2**)[1] with trifluoroacetic acid in chloroform at room temperature afforded a single adduct, **2a**, which arose solely from the *d,l*-dimer, leaving unreacted *meso*-dimer behind, which could be recovered in nearly pure form. When a solution of isomerically pure **1** in trifluoroacetic acid-chloroform was refluxed, a spiro compound, **1a**, was produced (Scheme 1). Electrophilic bromination of **2** also was studied. When isomerically pure **2** was reacted with excess Br_2-CCl_4 solution at room temperature, a single adduct, **2b**, was isolated. The *meso*-dimer, **1**, also reacted with excess Br_2-CCl_4 solution at room temperature, and the product obtained was not a 1,2-addition product but instead was found to be rearranged spiroketone **1b** (Scheme 1).[2]

The observation is remarkable in that the two stereoisomers, differing only in the axial chirality, showed such contrasting behaviours towards electrophiles. Since the stereoelectronic effect is apparently absent, we sought a steric explanation, using MM2[3] and AM1[4] methods.

Computational Techniques

MM2 calculations were performed by using a packaged program, BIGSTRN-3.[5] MM2-parameters for carbocation were taken from the work of Müller and Mareda.[6] A locally

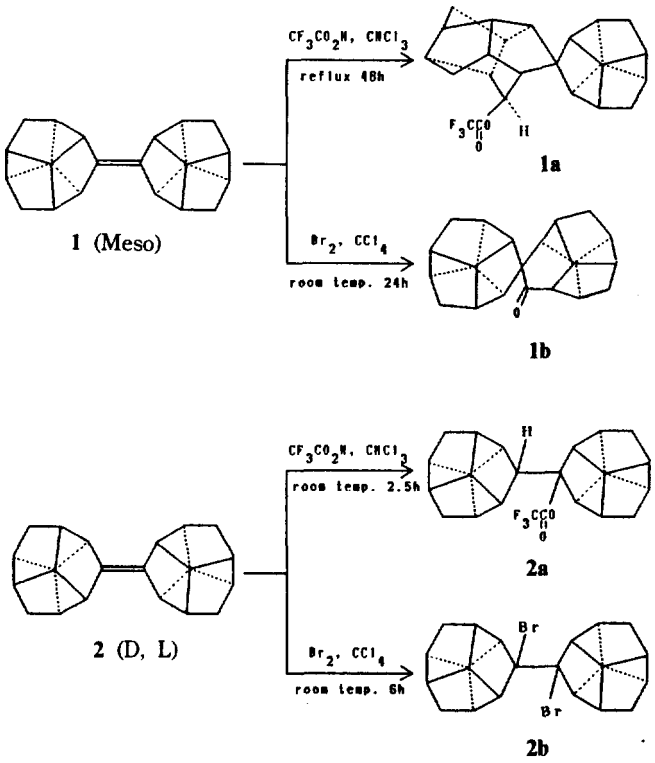

Scheme 1.

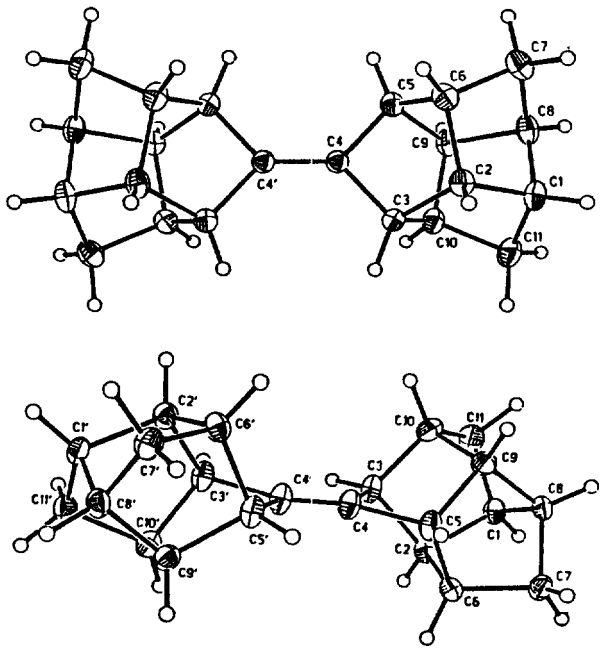

Figure 1. Structure drawing of **1** (Top) and **2** (Bottom).

Table 1. Standard Deviations of Differences Between the Observed (X-ray) and Calculated Structural Parameters for **1** and **2**

		MM2 (85)	AM1
C−C, Å	1	0.012	0.011
	2	0.014	0.013
C−C−C, deg	1	1.04	1.06
	2	1.15	1.15

updated modification of MOPAC (version 3.0) was used to perform AM1 calculations.[7] CRTEP drawings were made using Johnson's program.[8]

Results and Discussion

Dimers 1 and 2. As expected, both MM2 and AM1 reproduced the X-ray structures (Figure 1)[2] of the moderately strained olefins, **1** and **2**, quite well (Table 1). Double bonds are essentially planar in both **1** and **2**,[9] whereas the C=C bond lengths are somewhat shorter and the C−C(C=C)−C internuclear angles are very small than normal (Table 2). The small valence angles are clearly carried over from that of C_7 in norbornane,[11] and should have caused some increase in the *s*-character of the C_{sp^2}-C_{sp^2} σ-bond, thus leading to contraction of this bond.[12,13] This interpretation holds well for the series of olefins **1** to **4** (Table 2). As the C−C(=C)−C angle decreases from normal (110° for **4**) through 97° (for **1** and **2**) to 64° (for **3**), the C=C

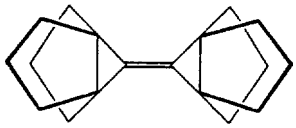

3

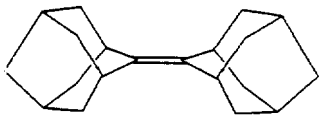

4

Table 2. $C(sp^2)-C(sp^2)$ Bond Lengths and $C(sp^2)-C(sp^2)-C(sp^3)$ Valence Angles of Several Tetra-substituted, Planar Ethylenes from x-ray Diffraction Analyses. The Number in Parenthesis is the Standard Devistion of Error in the Last Digit

Compound	Pt. Group	C=C, Å	<C−C(=C)−C, deg	Ref.
meso- **1**	C_{2h}	1.328(3)[a]	97.0(1)[b]	2
d,l- **2**	C_2	1.322(2)[c]	96.6(1)[d]	2
3	C_2	1.307(3)	63.6(2)	[e]
4	D_{2h}	1.336(4)	110.4(2)	[f]

[a] 1.332 (MM2), 1.320 (AM1). [b] 98.4 (MM2), 98.0 (AM1). [c] 1.332 (MM 2), 1.320 (AM1). [d] 98.4 (MM2), 98.0 (AM1). [e] Werner, P.; Chang, S.-C.; Powell, D. R.; Jacobson, R. A. *Tetrahedron Lett.*, **22**, 533 (1981). [f] Swen-Walstra, S. C.; Visser, G. J., *J. Chem. Soc., Chem. Commun.*, 82 (1971).

Table 3. Steric Energies (MM2) of D_3-tris-homocubylidene-D_3-trishomocubane (**1** and **2**, kcal/mol, 25°)

	1	**2**
Stretch	4.37	4.38
Bend	65.25	65.22
Str.-bend	−3.05	−3.05
VDW 1, 4	7.95	7.95
VDW Other	−5.74	−5.72
Torsion	44.17	44.19
Dipole	0.36	0.36
Sum	113.31	113.32

bond length indeed decreases from 1.34 to 1.31 Å. Hence, the structural features about the double bond are interpretable. However the effect of hybridization should influence **1** and **2** to the same extent, therefore these features cannot be responsible for the present problem.

Simulation of Earlier Reaction Paths. It is clear from the foregoing that differences between the reactivities of the C=C double bonds in **1** and **2** toward electrophiles (Scheme 1) cannot be ascribed to structural differences. Hence, We look to steric factors in order to explain these reactivity differences. Our interpretation of the observed reactivity differences, which is based upon the results of molecular mechanics (MM2)[3] calculations, is described below.

Several precautionary steps have been followed before we attempted to simulate the reaction. First, the geometries of **1** and **2** were optimized by using MM2, and the results were compared with the corresponding X-ray structures. The MM 2-derived structural parameters for **1** and **2** agreed closely with the corresponding experimental values (see above).

The MM2-derived steric energies of **1** and **2** are compared in Table 3. The energy distributions in both stereoisomers are virtually identical. The relatively high total steric energy arises primarily from angle bending and torsional factors. The former effect is dominated by the compressed methylene C−CH_2−C bond angles and the compressed C(3)-C(4)-C(5) bond angles (*vide supra*). High torsional energy content is typical feature of cage molecules.

The possibility that there may be some difference between

the extent of steric interference presented by β-protons in **1** and **2** toward the entering (solvated) electrophile also was considered explicitly. However, when the appropriate molecular modeling techiniques were applied to **1** and **2**, no significant difference in this regard could be found.

Finally, the relative stabilities of the intermediate carbocations (represented by protonated products **1-H**$^+$ and **2-H**$^+$, derived *via* protonation of **1** and **2**, respectively) were considered. If indeed a large difference existed between the stabilities of these two carbocations, the more stable intermediate should afford the predominant product. Initial geometries were established by attaching a proton to one of the two sp^2 C=C carbon atoms, and resulting species was geometry optimized with MM2. Full rotation-optimization calculations around the pivotal bond revealed only one outstanding energy minimum for both **1-H**$^+$ and **2-H**$^+$. The energy difference between these two minima is less than 0.2 kcal/mol. Hence, this factor cannot account for the observed difference between the reactivities of **1** and **2** toward electrophiles.

An interesting observation resulted from these calculations. The torsion angle, ω, between the newly formed C−H bond on the front carbon atom (see **5**) and the carbocation plane (defined by C−C−C on the back carbon atom) in **1-H**$^+$ decreased from an initial value of 90° to 58° during energy minimization. However, the corresponding torsion angle in **2-H**$^+$ remained virtually orthogonal throughout this process. This geometrical difference affords an important clue to understanding the origin of the observed difference between the reactivities of **1** and **2** toward electrophiles (*vide infra*).

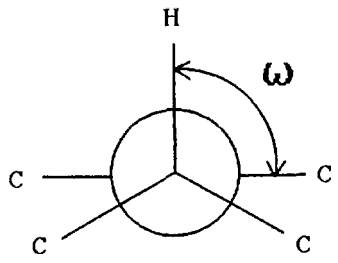

5

Since none of the structural or steric factors thus far considered can account for the observed reactivity difference, we concluded that the source of contrasting reactivity must originate *prior to* electrophilic attack on the substrate. Accordingly, an attempt was made by utilizing MM2 to simulate the path taken by the electrophile as it approaches the C=C double bond of **1** and **2**.

As a first approximation, the solvated electrophile was considered to be a sphere of positive charge. However, the effective van der Waals radius, r_o, and Buckingham-Hill hardness coefficient, ε, are difficult to estimate for this model. The Stokes radius of Li^+ in water (*i.e.*, 2.38 Å)[14] provides a hint regarding the effective magnitude of r_o of a solvated proton, but it should be considerably larger in chloroform *vis-à-vis* water as solvent. The value of ε in the Buckingham-Hill potential used in MM2 ranges between 0.1 and 0.5 kcal/mol for common atoms. Base upon this meager information, a number of combinations of r_o and ε were tested (*i.e.*, $4<r_o<6$ Å and $0.2<\varepsilon<2$). It turned out that the qualitative features

Table 4. Net Atomic Charges (AM1) of *meso* and *d,l*-D_3-trishomocubylidene-D_3-trishomocubane (**1** and **2**)

1	C1; −0.1177, C2; −0.1055, C3; −0.0797, C4; −0.0937, C5; −0.0798, C6; −0.1105, C7; −0.1573, C8; −0.1177, C9; −0.1055, C10; −0.1105, C11; −0.1572, H1; 0.1093, H2; 0.1055, H3; 0.1130, H5; 0.1130, H6; 0.1126, H7a; 0.0886, H7b; 0.0886, H8; 0.1091, H9; 0.1056, H10; 0.1125, H11a; 0.0885, H11b; 0.0887
2	C1; −0.1177, C2; −0.1055, C3; −0.0797, C4; −0.0936, C5; −0.0798, C6; −0.1105, C7; −0.1573, C8; −0.1177, C9; −0.1056, C10; −0.1106, C11; −0.1573, H1; 0.1092, H2; 0.1054, H3; 0.1130, H5; 0.1130, H6; 0.1128, H7a; 0.0885, H7b; 0.0887, H8; 0.1092, H9; 0.1055, H10; 0.1127, H11a; 0.0885, H11b; 0.0888

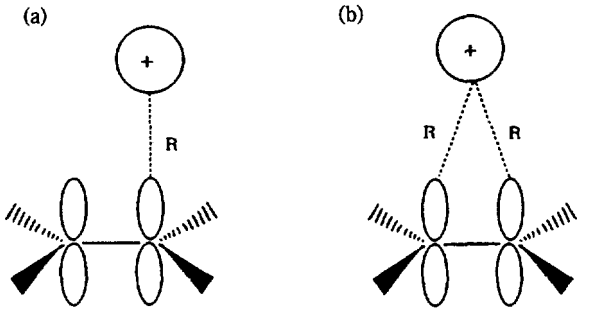

Scheme 2.

of the calculational results are not critically sensitive to the choice of these parameters. Accordingly, the discussion that follows is based upon results that were obtained by using $r_o=5$ Å and $\varepsilon=0.5$ kcal/mol.

The solvated electrophile was treated as a point charge when calculating electrostatic interactions between the approaching electrophile and C=C double bond in the substrate. Atomic charges were obtained from AM1 calculations of **1** and **2** (Table 4). These values were held invariant during the simulation calculations.

Protonation. The solvated proton was placed initially 10 Å above the plane that contains the C=C bond in **1** and **2**, and the composite was geometry-optimimzed for a given fixed distance, R, between the center of the spherical model of the solvated proton and C(4), *i.e.*, one of the sp^2-hybridized carbon atoms in the substrate (Scheme 2a). The distance R then was decreased in 1 Å decrements, and geometry-optimization was repeated at each fixed distance.

The distance $R=4$ Å turned out to be the critical distance beyond which composite geometries could not be optimized due to aggregate strain effects. Relavtive energies, $\Delta E=E(\mathbf{1})-E(\mathbf{2})$, are plotted against R in Figure 2. Initially, the total ΔE decreases as R is decreased from 10 Å to 6 Å but increases thereafter as R is further decreased. Steric component analysis indicates that the initial decrease in ΔE is due to an increase in the torsional energy of **2** relative to **1**. The subsequent increase in ΔE that occurs at $R<6$ Å is due at first to an increase in nonbonded repulsion in **1** (6 Å$>R\geq$ 5 Å) and then results from an increase in torsion energy in **1** (from $R=5$ Å down to $R=4$ Å, the critical distance).

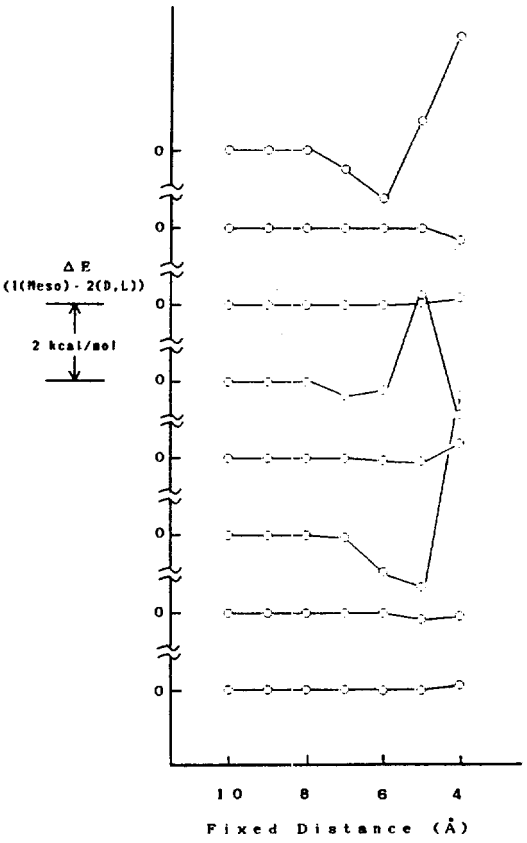

Figure 2. Changes in the relative MM2-steric energies, $\Delta E = E(\mathbf{1}) - E(\mathbf{2})$, kcal/mol, with decreasing electrophile-substrate distance R. Here, R is the distance (in Å) between the solvated proton and an sp^2-hybridized carbon atom in the substrate. Curves represent (from top to bottom): total steric energy, stretch-bend cross-term energy, charge interaction energy, nonbonded interaction energy, out of plane angle deformation energy, torsional energy, angle bending energy, and stretching energy.

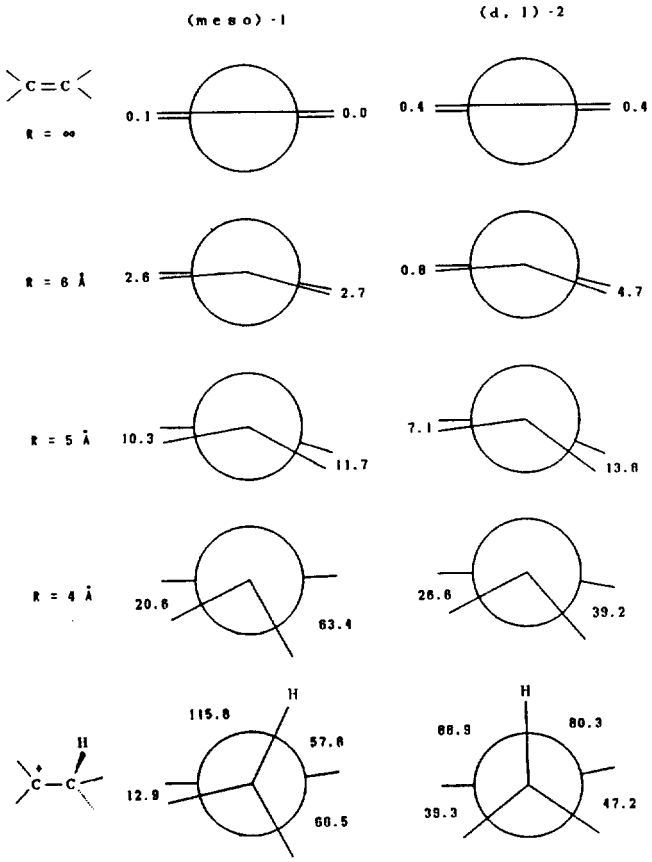

Figure 3. Newman projections along the C=C double bond in **1** and **2**, as the solvated model electrophile approaches the sp^2-hybridized carbon atom from above the plane of C=C double bond. See caption to Figure 2 for the definition of R.

The increased torsional strain in **2** *vis-à-vis* **1** that occurs at $R = 4$ Å is, in our opinion, the most important single factor that contributes to the observed difference between the reactivities of **1** and **2** toward electrophiles. This point can be appreciated further by inspection of Figure 3. A series of Newman projections shown therein illustrates the changes in carbon geometry that occur during the approach of H^+ to within 4 Å of one of the two doubly-bonded carbon atoms in **1** and in **2** (enroute to formation of the corresponding carbocation).

Common to **1** and **2**, both of the doubly bonded carbon atoms undergo pyramidalization with approach of the proton (model). Pyramidalization continues at the carbon atom that is undergoing protonation (*i.e.*, the "front" carbon atom) at distances $5 \geq R \geq 4$ Å. However, during this process, the "rear" carbon atom appears to recover some of its original planarity. Concomitant with the out-of-plane deformation (*i.e.*, pyramidalization), twisting also occurs. The fact that twisting is happening in **1** does not become evident until $R = 4$ Å is reached, at which point a large, clockwise rotation of the front carbon atom relative to the rear carbon becomes clearly visible (see Figure 3), thereby dramatically increasing the torsional energy content of the double bond. In contrast to this result, small twisting in **2** can be seen clearly at all values of R studied (Table 5).[15]

Table 5. Out-of-plane Deformation (Ψ) and Twist Angle (ϕ)[a] of Double Bond ($C_F = C_R$) in **1** and **2** Caused by the Approach of Solvated Proton Model Toward Carbon Atom C_F.[b]

R, Å	1 (*meso*)			2 (*d, l*)		
	Ψ_F	Ψ_R	ϕ	Ψ_F	Ψ_R	ϕ
6	17.33	−12.10	0.04	20.37	−14.86	1.95
5	40.36	−18.32	0.68	44.41	−23.67	3.23
4	82.46	1.54	21.38	76.67	−10.95	6.29
Carbonium ion						
(MM2)	74.80	6.60	27.83	75.79	−10.73	3.98
(AM1)	66.76	5.24	12.40	66.61	−3.18	6.88

[a] Based on Ermer's definition, see ref. 10. [b] The atom C_F being approached by proton is the front one in Figure 3. All numbers are given in degrees.

It is worthwhile to speculate upon the transition state that lies betwen: (i) the model in which approach of the proton toward the C=C double bond in the substrate has reached $R = 4$ Å and (ii) the optimized structure of carbonium ions **1**-H^+ and **2**-H^+ (see Figure 3, bottom). The most striking structural difference between carbonium ions **1**-H^+ and **2**-

H^+ is the fact that the twisting that is apparent in the model for **1**, $R=4$ Å remains or even has progressed as the transition state that leads to the carbonium ion is traversed. As a result, **1**-H^+ adopts a conformation in which the newly formed C−H bond on the front carbon atom is roughly "planar" with respect to the rear carbocationic center. In contrast to this result, **2**-H^+ adopts a conformation in which the newly formed C−H bond is roughly "orthogonal" to the plane of the rear carbocationic center.[16]

We interpret the foregoing results as follows: As the electrophile approaches from one side of the C=C double bond in the substrate, an out-of-plane deformation occurs that quickly narrows the gap between the two trishomocubylidene moieties on either side of the double bond. During this process, **2** is able to minimize any increase in total strain by introducing a small twist that eventually disappears into the orthogonal conformation of the carbonium ion, **2**-H^+. However, this option is not available to **1**. Consequently, the double bond in **1** is forced to twist toward the planar conformation of the corresponding carbonium ion, **1**-H^+. In so doing, nonbonded repulsions between γ- and γ′-hydrogen atoms on the back side of the double bond are reduced. Hence, twisting in **1** proceeds to some extent (at $R=4$ Å), but this movement must be energetically too costly to proceed. Consequently, while **2** smoothly achieves protonation, **1** encounters less resistance by undergoing instead antiperiplanar 1,2-shift from one of the pyramidalizing carbon bonds to the incipient cation center in the manner shown in **6**.

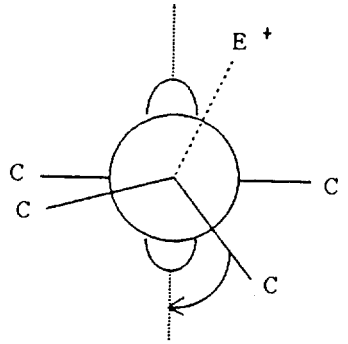

6

Bromination. The bridged bromonium ion model[17] shown in Scheme 2b was studied initially. In view of the insensitivity of qualitative features of the simulation to the size and hardness of the solvated electrophile mode (*vide supra*), we used the same radius and hardness constants for the solvated bromonium ion as had been employed previously for the solvated proton. The resulting bromonium ion model was placed on a line that passes through the center of the C=C double bond and is perpendicular to the plane of the double bond. The composite thereby obtained was geometry optimized while the model electrophile was constratined at a point equidistant from the termini of the C=C double bond. This results in C_S symmetry for the **1**+Br^+ composite and C_2 symmetry for **2**+Br^+.

Due to the symmetry conservation rule,[18] the composite **1**+Br^+ maintained its plane of symmetry throughout geometry optimization at all R values studied. No freedom to twist the double bond exists in this model as had been possible

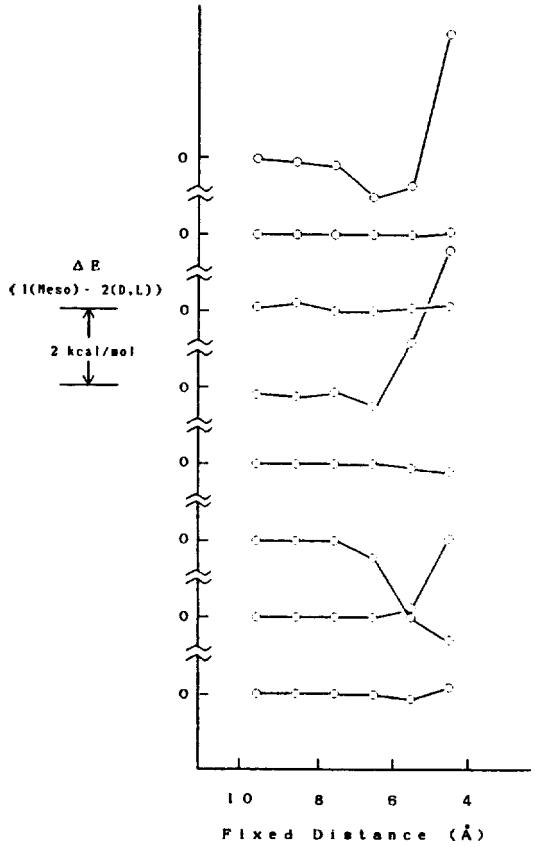

Figure 4. Changes in the relative MM2-steric energies, $\Delta E=E(1)-E(2)$, kcal/mole, with decreasing Br^+-substrate distance, R. See caption to Figure 2 for the explanation of curves.

in the corresponding protonation model. Likewise, the initial C_2 axis persists throughout the corresponding **2**+Br^+ process. In both composites, out-of-plane deformation occurred, and steric energy increased rapidly as R was decreased to 4.5 Å. Geometry optimization failed beyond this critical distance (*i.e.*, for $R<4.5$ Å). Total energy changed with decreasing R in a manner similar to that which was encountered for the corresponding protonation of **1** and **2**. Initially, the **2** composite is destabilized relative to the corresponding **1** composite until R reaches 5.5 Å due to torsional strain effects. However, the **1** composite becomes rapidly destabilized (relative to the **2** composite) as R is decreased to 4.5 Å due to the cumulative effects of nonbonded repulsion and angle strain.

Beyond this point, nothing can happen unless the initial symmetry constraints are removed. Conceptually, our model must now switch from the "bridged" composite (Scheme 2b) to the "single-footed" structure (Scheme 2a), and, at that point, bromination is expected to proceed in a manner that is closely analogous to the mechanism discussed earlier for protonation. Results were analyzed and summarized in Figure 4 and 5.

We conclude with cautionary note. The large out-of-plane deformation of the C=C double bond that we find herein is rarely seen except in the case of such highly strained molecules as *trans*-cyclooctene and the anti-Bredt alkenes.[10] The unexpected observation of large out-of-plane deforma-

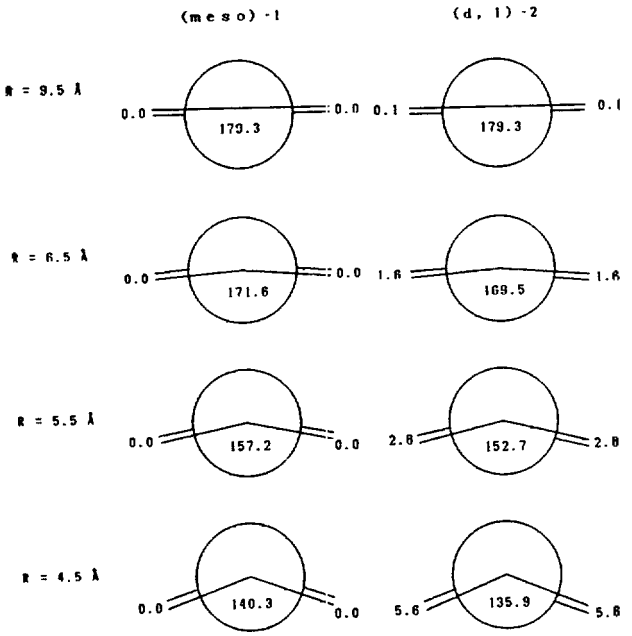

Figure 5. Newman projections along the C=C double bond in **1** and **2**, as Br^+ approaches the sp^2-hybridized carbon atoms from above the plane of the C=C double bond. See caption to Figure 2 for the definition of *R*.

tions may simply reflect the fact that all other carbon-carbon bonds in **1** and **2** are held rigidly within their respective cage structures and cannot bend. Comparison between the results obtained *via* MM2 and AM1 calculations (described in Table 5) suggests that the former method appears to exaggerate the out-of-plane deformations. For this reason, we are reluctant to claim that the early stages of electrophilic attack on **1** and **2** are described precisely by our MM2 computation that employs the solvated proton model. Nevertheless, we believe that the foregoing explanation should be qualitatively valid, as the nature of the steric effects invoked in our explanation should be independent of the computational methods that were employed.

Acknowledgement. We thank Professor A. P. Marchand, Department of Chemistry, University of North Texas, for suggesting the problem. Partial cost of this research was defrayed by a Grant-in-Aid for Scientific Research administered by the Ministry of Education, Science and Culture of Japan.

References

1. For absolute configuration of D_3-trishomocubane parts depicted in structures **1** and **2**, see, G. Helmchen and G. Staiger, *Angew. Chem.*, **89**, 119 (1977).
2. A. P. Marchand, G. M. Reddy, M. N. Deshpande, W. H. Watson, and A. Nagl, "*Synthesis and Reactions of meso- and d,l-D_3-Trishomocubylidene-D_3-trishomocubanone*", Long Abstract for 197th National ACS Meeting, Dallas, TX, April 9-14, 1989.
3. U. Burkert and N. L. Allinger, "*Molecular Mechanics*", ACS Monograph 177, American Chemical Society, Washington, DC, 1982.
4. M. J. S. Dewar, E. G. Zoebisch, E. F. Healy, and J. J. P. Stewart, *J. Am. Chem. Soc.*, **107**, 3902 (1985).
5. R. B. Nachbar, Jr. and K. Mislow, QCPE No. 514, BIGSTRN-3, 1986.
6. P. Müller, J. Mareda, *Tetrahedron Lett.*, **25**, 1703 (1984).
7. M. Togasi, J. M. Rudzinski, Z. Slanina, E. Ōsawa, and T. Hirano, *QCPE Bull.*, 7, 8 (1987).
8. C. K. Johnson, *ORTEP-II*, ORNL-5138, Oak Ridge National Laboratory, Oak Ridge, TN, 1976.
9. The twist angle as well as out-of-plane deformation of the double bond, according to the definition of Ermer,[10] are less than 0.2 degree.
10. O. Ermer, "*Aspeckte von Kraftfeldrechnungen*", Wolfgang Baur Verlag, München, 1981, Chapter 4.
11. E. Ōsawa, D. A. Barbiric, O. S. Lee, Y. Kitano, S. Padma, and G. Mehta, *J. Chem. Soc., Perkin Trans. II*, 1161 (1989).
12. O. Ermer and Lex, *J. Angew. Chem. Int. Ed. Engl.*, **26**, 447 (1987).
13. R. Gilardi, M. Maggini, and P. E. Eaton, J. Am. Chem. Soc., **110**, 7232 (1988).
14. R. E. Nightingle, *J. Phys. Chem.*, **63**, 1381 (1959).
15. It is interesting to note that the initial pyramidalization that occurs at the doubly bonded carbon atoms indicates the formation of a weak π-complex:

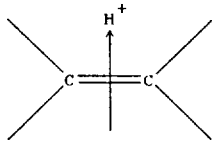

This "observation by molecular mechanics" stands in conflict with the belief held generally that protonation does not proceed *via* a bridged intermediate. See e.g., T. H. Lowry and K. S. Richardson, "*Mechanism and Theory in Organic Chemistry*", 2nd Ed., Harper and Row, New York, p. 509 (1981).
16. For the definition of "planar" and "orthogonal" conformations, see, e.g., P. J. Breen, J. A. Warren, E. R. Bernstein, and J. I. Seeman, *J. Am. Chem. Soc.*, **109**, 3453 (1987).
17. S. H. Pine, "*Organic chemistry*", 5th Ed., McGraw-Hill, Tokyo, p. 525 (1987).
18. O. Ermer, *Tetrahedron*, **31**, 1849(1975).